Accepted Manuscript

Modelling of textile composites with fibre strength variability

M.Y. Matveev, A.C. Long, I.A. Jones

PII: S0266-3538(14)00345-5
DOI: http://dx.doi.org/10.1016/j.compscitech.2014.09.012
Reference: CSTE 5940

To appear in: *Composites Science and Technology*

Received Date: 19 August 2014
Accepted Date: 21 September 2014

Please cite this article as: Matveev, M.Y., Long, A.C., Jones, I.A., Modelling of textile composites with fibre strength variability, *Composites Science and Technology* (2014), doi: http://dx.doi.org/10.1016/j.compscitech.2014.09.012

MODELLING OF TEXTILE COMPOSITES WITH FIBRE STRENGTH VARIABILITY

M. Y. Matveev*, A. C. Long, I. A. Jones

Polymer Composites Group, Faculty of Engineering, Division of Materials, Mechanics and Structures, University of Nottingham, University Park, Nottingham, NG7 2RD, UK

** Corresponding author: Mikhail.Matveev@nottingham.ac.uk, tel. +441159514147*

Abstract

Scatter in composite mechanical properties is related to variabilities occurring at different scales. This work attempts to analyse fibre strength variability numerically from micro to macro-scale taking into account the size effect and its transition between scales. Two micro-mechanical models based on the Weibull distribution were used within meso-scale finite element models of fibre bundles which were validated against experimental results. These models were then implemented in a meso-scale model of an AS4 carbon fibre plain weave/vinyl ester textile composite. Monte Carlo simulations showed that fibre strength variability has a limited effect on the strength of the textile composite at the meso-scale and introduces variability of less than 2% from the mean value. Macro-scale strength based on the predicted meso-scale distribution was lower than the strength of the composite without variability by 1-4% depending on the model. The presented multi-scale approach demonstrates that a wide fibre strength distribution leads to a narrow distribution of composite strength and a shift to lower mean values.

Keywords: A. Textile composites, B. Mechanical properties, C. Multiscale modelling

1. Introduction

Composite mechanical properties are highly scattered due to the presence of variabilities [1], e.g. the tensile strength of unidirectional (UD) composites can have coefficients of variation (CoV) of up to 5% [2]. Defects induced by manufacturing (e.g.

yarn waviness or variable ply placement) or variations in constituent properties affect composite properties. According to the multi-scale approach, uncertainties are divided into groups by length scale [2]. Micro-scale variabilities include packing of fibres within yarns, fibre waviness [3], voids between fibres and variability of constituent properties; meso-scale variabilities include variation of yarn path [4], size and shape of yarn cross-section, nesting and voids between yarns. All of these cause variations in local moduli (and therefore global stiffness), local strength (hence global strength) and local component shape distortions (hence global geometry), and it is not known *a priori* which of these are significant. Variability of fibre strength is well-known to affect composite properties and is well-studied [5]. However, no published studies explicitly link the distribution of fibre strength to the strength distribution of a woven composite.

Many analytical and numerical methods are based on the multi-scale approach, whereby a complex structure is divided into hierarchical sub-structures according to characteristic length. A heterogeneous medium at one scale is replaced by a homogeneous medium with the same properties at a higher scale. Homogenisation is usually based on the assumption of ideal periodicity at all levels and subsequent representation of a composite as a periodic unit cell. This approach has shown good results [6-8] despite controversy regarding the variability for real structures.

At the micro-scale the strength of single fibres can have a CoV of up to 20% and has a strong length dependence (strength can drop by 10% when length is increased by a factor of 10) [9]. This dependency and distribution are usually described by a two-parameter Weibull distribution with a length scale effect [5]. However, additional parameters are often required for correct description of the length effect [9].

The next step in multi-scale modelling is prediction of the strength of an impregnated fibre bundle or UD composite at the meso-scale. Several approaches can be considered. The Equal Load Sharing (ELS) concept postulates that the load from a broken fibre is equally distributed over all surviving fibres. This was used by Daniels [10] to derive mean strength and its distribution for an unimpregnated fibre bundle. A development of the model known as chain-of-bundles was employed for prediction of the strength of long fibre composites [11]. A drawback of this concept for an impregnated bundle is that it does not account for the unequal redistribution of stresses between fibres. GLS (Global Load Sharing) models assume an unloading zone at each side of fibre breakage. Theoretical predictions with various modifications are possible for a regular fibre arrangement. It was shown that both ELS and GLS models give close results once correct normalising constants are chosen [5]. Strength predicted by both approaches can be approximated by a normal distribution [5]. Unlike the ELS, the Local Load Sharing (LLS) concept assumes that the load from a broken fibre is distributed unequally to a number of neighbouring fibres according to a sharing rule [12, 13]. The number of neighbouring fibres that take the load depends on the properties of fibres and matrix and on the chosen theory. A number of analytical LLS models [5, 14] are able to predict final strength and its distribution. Computational LLS enables direct numerical simulations to be performed. Okabe and Takeda [15] used a spring model in conjunction with a shear lag law to simulate the strength of UD composites. On the other hand, recent research [16] shows the importance of realistic geometry (i.e. fibre packing) in predicting the stress-strain state of a UD composite in the case of fibre breakage. Finite element (FE) analysis was used to obtain the strength of a bundle of randomly packed fibres whose strength followed a Weibull distribution [17]. These models were able to capture the process of damage propagation or a realistic stress-strain state of the fibre array during fibre failure. However, an implementation of these micro-scale models at the meso-scale is not feasible.

The next step is meso-scale modelling of textile composites using properties obtained at the previous stage. Ismar et al [18] modelled an SiC/SiC woven composite with variability of yarn strength using FE analysis and a Monte Carlo method, varying strength in every element following a Weibull distribution and implementing a size effect. This showed the significant influence (about 10% reduction when a Weibull shape parameter was halved) of variability in impregnated bundle strength on tensile strength of woven composites. However, this study did not report standard deviation of final strength for a given distribution and predictions were not based on the distribution of single fibre strength.

This paper applies a multi-scale modelling approach for a textile composite with variability in fibre properties. Fibre bundle strength models were chosen and validated against experimental data for UD composites based on single fibre strength distributions. The models ensured correct transition between scales taking into account the size effect which is critical for meso-scale FE modelling. Using the fibre bundle strength model, stochastic FE simulations were performed to determine the distribution of composite mechanical properties.

2. Variability models

2.1. Strength model of single fibre

The Weibull distribution is often used for prediction of single fibre strength [5, 19]. Taking into account the length effect, a fibre of length L under tensile stress σ has a cumulative failure probability P_f given by

$$P_f = 1 - \exp(-(L/L_0)(\sigma/\sigma_0)^{\rho}) \quad (1)$$

where σ_0 is the Weibull scale parameter, ρ the shape parameter and L_0 the gauge length.

However, it was found that this approach tended to overestimate the strength of some types of fibres of shorter length [9, 15, 20], and the experimental fibre strength distribution at different length scales is better described by [9]

$$P_f = 1 - \exp(-(L/L_0)^{\alpha}(\sigma/\sigma_0)^{\rho}) \quad (2)$$

where α is an additional parameter satisfying $0 < \alpha \leq 1$.

This empirical relationship was related to fibre-to-fibre variation of the scale parameter [9]. This was explored by Beyerlein and Phoenix [21] for a bundle consisting of four fibres. This approach, termed Weibull of Weibulls, was extended further by applying it to all fibres in the composite [22]. Then the cumulative probability of fibre failure, P_f, under loading stress σ is

$$P_f = 1 - \exp\left(-(L/L_0)\left(\sigma/\sigma_0^i\right)^{\rho'}\right) \quad (3)$$

where L is fibre length, L_0 is the reference gauge length, $\rho' = \rho/\alpha$ is a Weibull shape parameter and the Weibull scale parameter σ_0^i has a cumulative distribution P_{σ_0}

$$P_{\sigma_0} = 1 - \exp\left(-(\sigma_0^i/\bar{\sigma}_0)^m\right) \quad (4)$$

where m is a Weibull shape parameter and $\bar{\sigma}_0$ is a scale parameter. Curtin showed that eqs. (3) and (4) give a strength distribution close to that from eq. (2), but with parameters measured directly from single fibre tests. Eqs. (3) and (4) are used later to describe distribution of fibre strength in fibre bundles.

2.2. Strength model of impregnated fibre bundle

Analysis of failed UD composites shows that fibre damage tends to cluster before final failure [15]. Here it is assumed that in a full-scale FE model these clusters can be modelled as small bundles or domains (finite elements) whose strength is calculated using a theoretical model. Three approaches were employed for comparison: the ELS concept using direct calculations as described below, the ELS concept in its normal distribution approximation [5, 10] and the GLS concept in its approximation as a Gaussian process [5, 23, 24]. However, the entire approach effectively implements an LLS model due to stress redistributions in an FE model which follow element failure.

To find the strength of an individual element a bundle of N fibres is considered. For the ELS approach the stress S^i prior to i-th fibre failure is [10]:

$$S^i = \frac{V_f}{N}(N - i + 1)S_f^i + (1 - Vf)S_m', \tag{5}$$

where V_f is fibre volume fraction, $S_m' = E_m S_f^i / E_f$ is stress in the matrix at the fibre failure strain and S_f^i, $i = 1...N$ are the strengths of individual fibres, calculated with eqs. (3) – (4). The second term in eq. (5) accounts for matrix stress contribution.

Eq. (5) defines a series of stresses corresponding to progressive failure of fibres in the bundle. The ultimate bundle strength is then defined as max(S^i). It was shown by Daniels [10] that the strength of an infinitely large bundle tends to a normal distribution.

A more realistic GLS concept was also employed as an alternative method for determining the bundle (finite element) strength. It assumes that load is redistributed through shear after a single fibre break. The strength distribution along the length of the bundle predicted by this concept was shown to be asymptotically close to a Gaussian process which mean, standard deviation and covariance function can be found in [23]. The comparison with the ELS model was shown to be possible when the correct characteristic strength is used for the GLS model [5].

It should be noted that, in all the models, fibres within the impregnated bundle are assumed to be perfectly aligned with the finite element edges and therefore the size of the element defines its strength through the length and size of the fibre bundle.

2.3. Damage model

A continuum damage mechanics (CDM) approach was used for the impregnated bundle [25]. This suggests linear behaviour until damage initiation, followed by gradual degradation of elastic properties. Five failure modes were considered: longitudinal tension/compression, transverse tension/compression and transverse shear. Damage initiates when one of the damage variables D_i defined by eqs. (7) – (9) exceeds 1. Stress tensor components σ_{ij} are calculated in local coordinates where "1" is the longitudinal fibre direction, and "2" and "3" are orthogonal transverse directions, which are equivalent due to transverse isotropy of an impregnated bundle.

$$D_1 = \max\left(\frac{\sigma_{11}}{F_{11}^t}, \frac{-\sigma_{11}}{F_{11}^c}\right) \tag{7}$$

$$D_2 = \frac{\sqrt{\sigma_{12}^2 + \sigma_{13}^2}}{F_{12}} \tag{8}$$

$$D_3 = \max\left(\frac{\max(\sigma_{2,}\sigma_3)}{F_{22}^t}, -\frac{\min(\sigma_{2,}\sigma_3)}{F_{22}^c}\right), \tag{9}$$

where σ_2 and σ_3 are principal stresses in the plane orthogonal to the fibre direction, F_{ij}^m are strengths of the impregnated bundle (yarn) where indices i, j = 1,2 correspond to directions and index $m = t, c$ stands for tension and compression.

After damage initiation, Young's and shear moduli E_i, G_{ij} of the yarn are given by:

$$E_1 = \begin{cases} E_1^0 & D_1 \leq 1 \\ 0.001E_1^0 & D_1 > 1 \end{cases} \tag{10}$$

$$E_2 = E_3 = E_2^0 \max\left(0.001, \min\left(P(\mathrm{D}_2), P(\mathrm{D}_3)\right)\right) \tag{11}$$

$$G_{12} = G_{13} = G_{12}^0 \max\left(0.001, \min\left(P(\mathrm{D}_2), P(\mathrm{D}_3)\right)\right), \tag{12}$$

where $P(D_i)$ is a damage factor function and is defined as

$$P = \left(1 - \frac{1}{\exp\left(-c_1 D_i + c_2\right)}\right). \tag{13}$$

From eq. (10) it can be seen that damage initiation in the longitudinal direction causes catastrophic failure. Transverse damage is assumed to propagate gradually, similar to Puck's theory [26]. Poisson's ratios remain unchanged. Constants c_1 and c_2 in eq. (13) were determined by Ruijter [25] and a ratio c_2/c_1 equal to 1.62 was found to give close agreement with experimental stress-strain curves for a plain weave composite under tensile load. Setting c_1 and c_2 to zero leads to abrupt degradation similar to [6, 8]. The ratio c_2/c_1 determines the damage variable D_i when properties are fully degraded and the appropriate elastic modulus becomes insignificantly low.

The matrix was assumed to be elastic prior to failure. Failure onset in the case of prevailing tensile behaviour was described by the von Mises criterion. Young's modulus degradation was described by a damage factor as in eq. (13). This was implemented in a UMAT user-defined material subroutine within Abaqus/Standard™.

2.4. Validation on tensile strength tests of impregnated tows and UD composites

The proposed model was validated on fibre bundles with different numbers of fibres. Statistical distributions often possess a strong size effect, therefore the model should be able to predict the correct behaviour of tows and UD composites of various lengths and numbers of fibres. All three approaches described in Section 2.2 were employed for full-scale FE modelling and results were compared. Published experimental results [15, 22, 27, 28] were used to validate the model.

For direct calculation of an ELS fibre bundle, the number of fibres in each finite element was found and fibre strengths were assigned following eqs. (3) and (4) using the length of the element as input parameter L. Then bundle strength was calculated as $\max(S^i)$ where S^i is defined by eq. (5). For alternative models (ELS and GLS), strength of elements was seeded using a normal distribution with mean and standard deviation as given in [5, 19, 23] using parameters listed in Table 1. The covariance function in the GLS distribution was found to be negligibly small and therefore strengths of neighbouring elements were assumed to be independent. The other properties of the impregnated bundle were found using the Chamis formulae [29]. Input data for the bundle strength model were taken from published sources, as listed in Table 1.

Using the above damage model, mesh convergence studies for a full scale model (overall length 20 mm) of a T700/Epoxy 12K impregnated fibre bundle were conducted for the three fibre bundle strength models. The strength of brick-shaped elements varied with mesh refinement reflecting change of length and number of fibres per element. Convergence of strength with refinement is shown in Fig. 1a, where each point is the average of 40 calculations and error bars represent one standard deviation. The Weibull plot and its parameters for experimental and predicted data are shown in Fig. 1b. The ELS model predicted a strength approximately 3% lower than the GLS model, which in turn was 1.5% lower than the experimental value. The difference between the direct calculations in the ELS model and its approximation were negligible. The distributions have the same Weibull shape parameter (lines are almost parallel, difference between shape parameters within 3% for both ELS and GLS approaches) but the experimental Weibull scale parameter is 5% higher than predicted using the ELS approach and 4% lower than predicted with the GLS model. Convergence studies for the full scale model of AS4/Epoxy were published earlier by the present authors [30].

Results of the Monte Carlo method coupled with FE damage analysis for two different composites are listed in Table 2. As expected, both versions of the ELS model yielded results in very close agreement. The GLS model predicted average strength 5% higher than that predicted with the ELS models but the standard deviation was about the same in absolute terms. In general, the proposed algorithms tend to underestimate the actual strength for UD composites while the "rule of mixtures" always overestimates it (when manufacturer's data are used within the equation $S_{uts} = V_f S_f + (1\text{-}V_f)E_m S_f/E_f$).

3. Finite element model of composite with fibre strength variability

3.1. Unit cell model of textile composite

A plain weave textile composite consisting of eight layers of AS4 reinforced vinyl ester [31] was used to investigate the influence of fibre strength on overall strength. TexGen software [32] and a voxel meshing technique [33] were used to generate an FE model of the composite. The unit cell is shown in Fig. 2, where geometric parameters were: L = 6.27 mm, H = 0.624 mm, h_y = 0.31 mm, w_y = 2.81 mm [31], giving a fibre volume fraction of V_f = 0.44 [31]. Constituent properties were: matrix Young's modulus E_m =3.45 GPa, Poisson's ratio v_m =0.35, strength σ_m=76 MPa, fibre Young's modulus E_f=221GPa and constant fibre strength σ_f =3930MPa. Other elastic properties and parameters for the variability model are listed in Table 1. Yarn effective moduli and strengths were found with the Chamis formulae with an intra-yarn fibre volume fraction of 63% [29]. The composite tested in [31] had no nesting between layers, therefore periodic boundary conditions [34] were applied to the unit cell in all three directions.

3.3. FE voxel model

The solution error is defined by the quality of the conformal tetrahedral mesh e.g. by the ratio of maximal element dimension and sine of maximum angle between element faces [35] or by the element aspect ratio [36]. However, conformal FE meshes of textile composite unit cells usually contain distorted elements in regions between yarns [33, 37] which will increase the solution error. This can be solved by use of a specially constructed geometry with yarns forced to touch each other in a pre-defined manner [38] or by introduction of an artificial clearance between yarns [7, 39]. Both methods allow generation of a good quality mesh but limit the creation of a realistic geometry. The mesh superposition [40] and domain superposition techniques [41] provide alternative ways to discretise a textile composite by meshing the textile and boundary domain separately and linking them during FE analysis. Although capable of good predictions for elastic properties, these techniques introduce a discontinuity in stresses and strains at the yarn/matrix interface which may affect strength predictions.

Meshing problems as discussed above are avoided using a voxel mesh technique [33]. A voxel mesh consists of rectangular cuboidal elements with element attributes defined by those at the voxel centroid. Mesh quality is known *a priori* and the mesh can be generated for any geometry without any artificial changes in textile geometry. On the other hand, the resolution (number of elements) of a voxel mesh, required to be high to achieve accurate representation of the textile geometry, is limited by computational costs. A voxel mesh can be locally refined [33] or a smoothing algorithm can be used to improve tow/matrix interface surfaces [37].

To validate the voxel approach, conformal and voxel meshes were generated for the same textile geometry. A vertical clearance between yarns was introduced to achieve a good quality conformal tetrahedral mesh. The periodic tetrahedral mesh was generated via TexGen which implements Delaunay tetrahedralization using TetGen software [42]. The gap introduced between yarns reduced overall fibre volume fraction and hence Young's modulus to 85% of the original value. Convergence of elastic modulus and initial failure strain are shown in Fig. 3a. Comparison of stress-strain curves presented in Fig. 3b shows that the voxel and conformal meshes give similar solutions for the considered materials and load case. This allows a highly refined voxel mesh to be used instead of a conformal mesh for later studies. All FE models in this study had 120000 nodes giving a compromise between analysis time and accuracy.

3.4. Effect of strength variability on textile composites

The influence of fibre strength variability on textile composite strength was studied using the unit cell model. The strength of each voxel was chosen according to the direct ELS and GLS approaches described above and AS4 fibre parameters are listed in Table 1. Stochastic simulations were performed for a mesh of the same size as for the model without variability. Experimental and predicted stress-strain curves for composites under tensile loading are shown in Fig. 4. Predicted final strength of 530 MPa for the composite without variability was above the experimental value of 480 MPa. However, predicted and experimental stress-strain curves were in relatively good agreement below the failure point. An interesting feature of both experimental and predicted stress-strain curves is a "knee" at a strain of about 1%. The FE simulations showed that the "knee" is preceded by development of large transverse cracks in transverse yarns together with minor shear damage in longitudinal yarns. Damage in transverse yarns "relaxes" the stress-strain state in longitudinal yarns allowing them to straighten to a degree which results in the "knee". After yarn straightening, the composite exhibits a modulus close to its initial value, since the contribution of transverse yarns to overall stiffness is minor. This "knee" is not present in the stress-strain curve on Fig. 3b as here the large matrix pockets introduced in this fictional composite prevented the behaviour described above.

The average final strength of the composite with fibre strength variability predicted with the ELS model was lower than that without variability due to the presence of weak fibres and hence elements with lower strength where damage is more likely to initiate. The distribution of final strengths is shown in Fig. 5. The original fibre strength distribution (Distribution 1) was varied to increase standard deviation by factors of two (Distribution 2) and three (Distribution 3) leaving mean fibre strength unaltered. Compared to the composite without variability, fibre strength variability decreased the composite's failure strength by 1.7% while for Distributions 2 and 3 was reduced by 5.6% and 15.7% respectively. Standard deviations of strength for these three cases were 6.0 MPa, 3.7 MPa and 3.4 MPa, respectively. These compare favourably with the experimental standard deviation of 7.3 MPa (for four specimens). Reduction in standard deviation with broadening fibre strength distribution can be explained considering the composite prior to final failure which occurs when several elements are damaged in the most highly stressed region of longitudinal yarns. In case of a wide fibre strength distribution it is highly probable that weak elements from the lower tail of the strength distribution will be present here and will trigger final failure.

Results of simulations using the GLS model were different from those obtained with the ELS model. First of all, the average final strength of the composite was found to be 1.9% higher than the value predicted with no variability, although the CoV was similar to that predicted with the ELS model and was equal to 1.2%.

However, in modelling of macro-scale damage, a composite with variability cannot be represented as a single unit cell due to the size effect, since larger specimens show lower strength compared to smaller samples [2]. This is often described by a weakest link approach based on a cumulative distribution function *G* for a chain of *n* links:

$$G(\sigma) = 1 - (1 - F(\sigma))^n \quad (14)$$

where *F* is the cumulative distribution function of the links' strength.

Strength predicted with eq. (14) over the number of links in the chain is shown in Fig. 6. For a chain consisting of 25 links compared to a single unit cell, strength is reduced by 2.7% which gives a strength of 507 MPa and 528 MPa at the gauge length of 160 mm (experimental specimen length [31]) for ELS and GLS models, respectively. The standard deviation is reduced by the same factor as the strength.

4 Discussion

The chosen models of impregnated fibre bundle strength were compared with experimental results. Mean values of strength predicted by the ELS and GLS models differed respectively by 6.3% and 1.5% from experimental data for a 12K bundle. Here the predicted strength distribution had a shape parameter close to the experimental one but Weibull moduli ere different. This could stem from the fact that experimental data for single fibre strength and bundle strength originated from different sources with no confidence of similar fibre treatment and therefore properties. Another possible source of error is the bundle strength models which do not take into account stress redistribution after single fibre failure and therefore predict reduced overall strength. Nevertheless, the proposed model has correctly captured the variation of bundle strength and has made it possible to estimate the effect of fibre strength variability on textile composite properties. The difference between predictions with different bundle models can be explained by the concept of the ELS model which is based on an "all or nothing" paradigm, resulting in lower bundle strength and higher standard deviation.

Comparison of a voxel mesh against a conformal mesh for a plain weave composite showed that under tensile loading a voxel mesh can be used instead of a conformal mesh but requires more elements for convergence. The CDM model showed adequate results in prediction of nonlinear response under tensile loading. However, it over-predicted final failure strength by 11% compared to experimental data.

Variability of fibre strength was shown not to have a dominant effect on composite strength at the meso-scale when only one unit cell is considered. For both models there were small changes in final strength with the GLS model predicting higher final composite strength and the ELS model predicting lower strength when compared to simulations without variability. It is worth noting that the CoV for both cases was approximately the same at 1.1%. However, broadening the distribution of fibre strength changed failure strength by 5% and 15% when the standard deviation of fibre strength was doubled and tripled, respectively. For a broader distribution of fibre strength, fibre damage initiated much earlier compared to the original distribution and this early damage initiation changed the shape of the stress-strain curve and decreased the standard deviation of the composite strength distribution.

The predicted CoV is lower than the CoV that sometimes observed in experimental results for composite materials. This poses a question as to the significance of other types of variability. Other possible sources (and differences between predicted and experimental results) are local geometrical distortions, manufacturing induced defects and effects such as stiffening of carbon fibre. The latter can decrease the final strength of a textile composite due to higher stresses at high strains and increase the CoV of strength of the composite due to additional variability in Young's modulus. However, more probably, the non-Hookean behaviour of carbon fibres will be outweighed by yarn straightening at low strain levels and damage propagation at high strain levels.

The macro-scale length effect was investigated using a weakest link model with link strength obtained from the unit cell strength distribution. A gradual decrease in composite strength was predicted with increase in composite length. Mean composite strength for a length of 160 mm was predicted to be 4.5% and 1% lower than that of a single unit cell without variability for the ELS and GLS approaches, respectively. However, the number of unit cells along the length is lower than the total number of unit cells in a specimen as specimen width and thickness are neglected in the model. Also, the weakest-link model neglects load redistribution between unit cells. Nevertheless, the trend of decreasing strength with increasing number of cells suggests that strength for a full sized model will be lower than predicted by the presented model and hence closer to experimental data.

5 Conclusions

Three fibre strength models were validated against experimental results for fibre bundles of different sizes. The difference between ELS and GLS models was within 5% in mean value and 10% in standard deviation. GLS yielded higher values than the ELS model which is expected as the latter is a more extreme case of load sharing between fibres. Models were then implemented in a FE model for a textile composite.

The textile composite was modelled by FE analysis using the voxel mesh technique and a CDM approach. The voxel mesh was validated against a conventional conformal mesh and shown to be acceptable. Stochastic simulations showed that fibre strength variability changed the final strength at meso-scale by 2% in comparison with predictions with no variability and introduced a CoV of about 1.1%.

The strength of the composite with a length of 160 mm, calculated using the weakest link approach and distributions predicted with ELS and GLS models, were respectively 4.5% and 1% lower compared to the strength of a single unit cell with uniform fibre strength distribution.

Acknowledgements

The authors would like to thank J. Heil and L. Harper for providing some of the experimental data presented in this paper. The University of Nottingham is gratefully acknowledged for its financial support via a studentship to Mikhail Matveev.

References

[1] Sriramula S, Chryssanthopoulos MK. Quantification of uncertainty modelling in stochastic analysis of FRP composites. Compos Pt A-Appl Sci Manuf. 2009;40(11):1673-1684.

[2] Wisnom MR. Size effects in the testing of fibre-composite materials. Compos Sci Technol. 1999;59(13):1937-1957.

[3] Yushanov SP, Bogdanovich AE. Fiber waviness in textile composites and its stochastic modeling. Mech Compos Mater. 2000;36(4):297-318.

[4] Endruweit A, Long AC. Influence of stochastic variations in the fibre spacing on the permeability of bi-directional textile fabrics. Compos Pt A-Appl Sci Manuf. 2006;37(5):679-694.

[5] Phoenix SL, Beyerlein IJ. Statistical Strength Theory for Fibrous Composite Materials. In: Kelly A, Zweben C, editors. Comprehensive Composite Materials, Oxford: Pergamon; 2000. p. 559-639.

[6] Blackketter DM, Walrath DE, Hansen AC. Modeling Damage in a Plain Weave Fabric-Reinforced Composite-Material. J Compos Tech Res. 1993;15(2):136-142.

[7] Ivanov DS, Baudry F, Van Den Broucke B, Lomov SV, Xie H, Verpoest I. Failure analysis of triaxial braided composite. Compos Sci Technol. 2009;69(9):1372-1380.

[8] Zako M, Uetsuji Y, Kurashiki T. Finite element analysis of damaged woven fabric composite materials. Compos Sci Technol. 2003;63(3-4):507-516.

[9] Watson AS, Smith RL. An Examination of Statistical-Theories for Fibrous Materials in the Light of Experimental-Data. J Mater Sci. 1985;20(9):3260-3270.

[10] Daniels HE. The statistical theory of the strength of bundles of threads. I. Proc R Soc Lon Ser-A. 1945;183(A995):0405-0435.

[11] Harlow DG, Phoenix SL. Chain-of-Bundles Probability Model for Strength of Fibrous Materials .1. Analysis and Conjectures. J Compos Mater. 1978;12(Apr):195-214.

[12] Newman WI, Phoenix SL. Time-dependent fiber bundles with local load sharing. Phys Rev E. 2001;63(2).

[13] Smith RL. A Probability Model for Fibrous Composites with Local Load Sharing. P Roy Soc Lond a Mat. 1980;372(1751):539-553.

[14] Pimenta S, Pinho ST. Hierarchical scaling law for the strength of composite fibre bundles. J Mech Phys Solids. 2013;61(6):1337-1356.

[15] Okabe T, Takeda N. Size effect on tensile strength of unidirectional CFRP composites - experiment and simulation. Compos Sci Technol. 2002;62(15):2053-2064.

[16] Swolfs Y, Gorbatikh L, Romanov V, Orlova S, Lomov SV, Verpoest I. Stress concentrations in an impregnated fibre bundle with random fibre packing. Compos Sci Technol. 2013;74:113-120.

[17] Mishnaevsky Jr L, Brøndsted P. Micromechanisms of damage in unidirectional fiber reinforced composites: 3D computational analysis. Compos Sci Technol. 2009;69(7–8):1036-1044.

[18] Ismar H, Schröter F, Streicher F. Influence of the fiber volume fraction and the fiber Weibull modul on the behavior of 2D woven SiC/SiC — a finite element simulation. Acta Mech. 2001;149(1):41-54.

[19] Mccartney LN, Smith RL. Statistical-Theory of the Strength of Fiber-Bundles. J Appl Mech-T Asme. 1983;50(3):601-608.

[20] Zhao FM, Okabe T, Takeda N. The estimation of statistical fiber strength by fragmentation tests of single-fiber composites. Compos Sci Technol. 2000;60(10):1965-1974.

[21] Beyerlein IJ, Phoenix SL. Statistics for the strength and size effects of microcomposites with four carbon fibers in epoxy resin. Compos Sci Technol. 1996;56(1):75-92.

[22] Curtin WA. Tensile strength of fiber-reinforced composites: III. Beyond the traditional Weibull model for fiber strengths. J Compos Mater. 2000;34(15):1301-1332.

[23] Hui CY, Phoenix SL, Ibnabdeljalil M, Smith RL. An Exact Closed-Form Solution for Fragmentation of Weibull Fibers in a Single Filament Composite with Applications to Fiber-Reinforced Ceramics. J Mech Phys Solids. 1995;43(10):1551-1585.

[24] Phoenix SL, Ibnabdeljalil M, Hui CY. Size effects in the distribution for strength of brittle matrix fibrous composites. Int J Solids Struct. 1997;34(5):545-568.

[25] Ruijter W. Analysis of mechanical properties of woven textile composite as functions of textile geometry PhD thesis. University of Nottingham, School of M3, 2008.

[26] Puck A, Schurmann H. Failure analysis of FRP laminates by means of physically based phenomenological models. Compos Sci Technol. 2002;62(12-13):1633-1662.

[27] Luchoo R, Harper LT, Bond MD, Warrior NA, Dodworth A. Net shape spray deposition for compression moulding of discontinuous fibre composites for high performance applications. Plast Rubber Compos. 2010;39(3-5):216-231.

[28] Feih S, Boiocchi E, Kandare E, Mathys Z, Gibson AG, Mouritz AP. Strength degradation of glass and carbon fibres at high temperature. 17th Internation Conference on Composite Materials, Ediburgh, UK2009.

[29] Chamis CC. Mechanics of Composite-Materials - Past, Present, and Future. J Compos Tech Res. 1989;11(1):3-14.

[30] Matveev MY, Long AC, Jones IA. Mechanical properties of textile composites with variability in micromechanical properties. 15th European Conference on Composite Materials, Venice, Italy2012.

[31] Ito M, Chou TW. An analytical and experimental study of strength and failure behavior of plain weave composites. J Compos Mater. 1998;32(1):2-30.

[32] Sherburn M. Geometric and Mechanical Modelling of Textiles PhD. University of Nottingham, School of M3, 2007.

[33] Kim HJ, Swan CC. Voxel-based meshing and unit-cell analysis of textile composites. Int J Numer Methods Eng. 2003;56(7):977-1006.

[34] Li SG, Wongsto A. Unit cells for micromechanical analyses of particle-reinforced composites. Mech Mater. 2004;36(7):543-572.

[35] Krizek M. On the Maximum Angle Condition for Linear Tetrahedral Elements. Siam J Numer Anal. 1992;29(2):513-520.

[36] ABAQUS 6.9 Documentation.

[37] Potter E, Pinho ST, Robinson P, Iannucci L, McMillan AJ. Mesh generation and geometrical modelling of 3D woven composites with variable tow cross-sections. Comput Mater Sci. 2012;51(1):103-111.

[38] Tang XD, Whitcomb JD. Progressive failure behaviors of 2D woven composites. J Compos Mater. 2003;37(14):1239-1259.

[39] Lomov SV, Ivanov DS, Verpoest I, Zako M, Kurashiki T, Nakai H, et al. Meso-FE modelling of textile composites: Road map, data flow and algorithms. Compos Sci Technol. 2007;67(9):1870-1891.

[40] Kurashiki T, Zako M, Nakai H, Imura M, Hirosawa S. Damage development of woven composites based on multi-scale analysis. ICCM-16, 2007.

[41] Jiang WG, Hallett SR, Wisnom MR. Development of Domain Superposition Technique for the Modelling of Woven Fabric Composites. Comp Meth Appl Sci. 2008;10:281-291.

[42] Si H, Gartner K. Meshing piecewise linear complexes by constrained Delaunay tetrahedralizations. Proceedings of the 14th International Meshing Roundtable. 2005:147-163.

Figure(s)

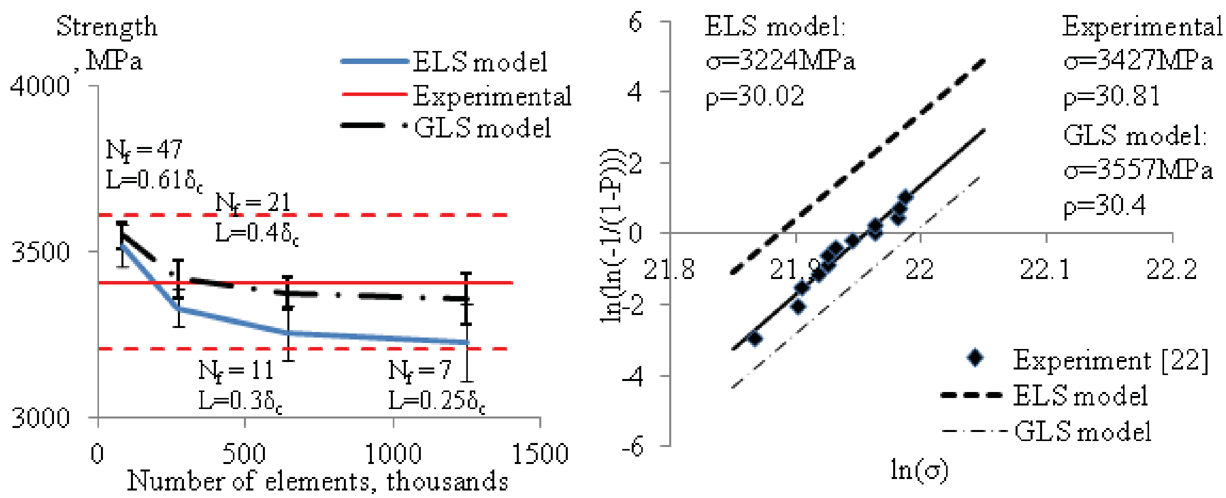

Figure 1. a) Convergence of FE solution with mesh refinement; b) Weibull plot for 12K impregnated fibre bundle of T700 fibres.

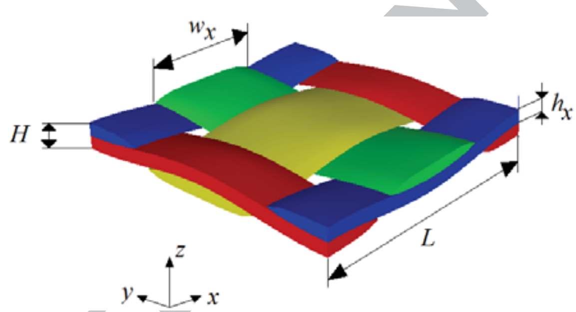

Figure 2. The unit cell of plain weave textile composite with removed matrix

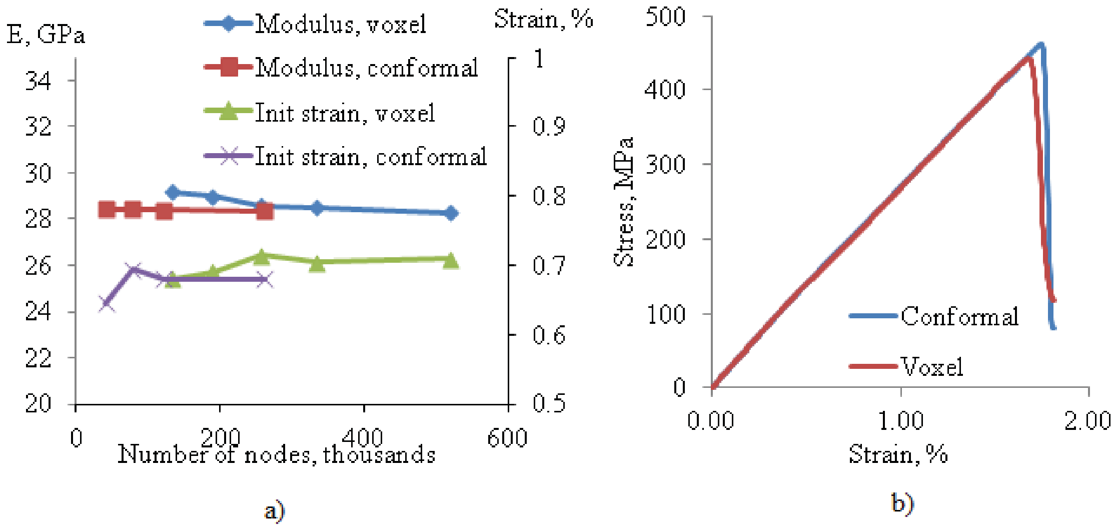

Figure 3. a) Convergence of voxel and tetrahedral meshes; b) Comparison of stress-strain curves for voxel and conformal mesh solutions

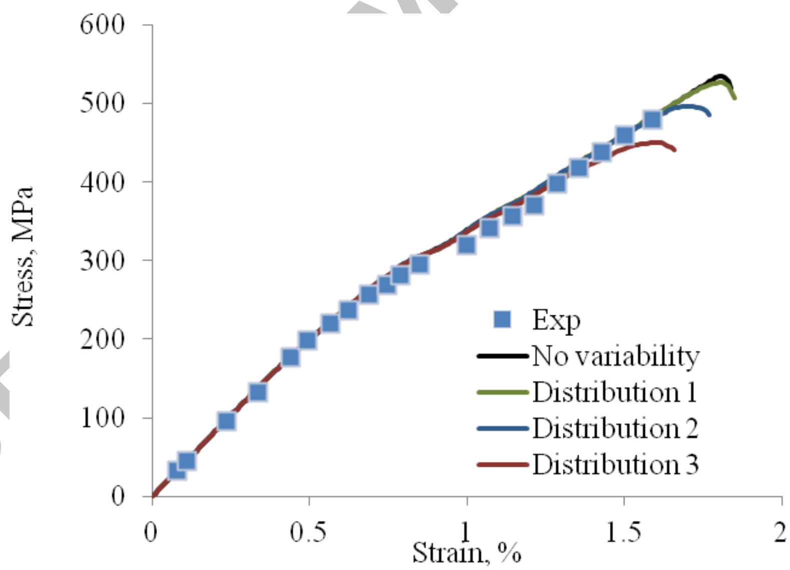

Figure 4. Experimental and predicted stress-strain curves (ELS model) for plain weave composite with and without variability; Distributions 1, 2 and 3 are original and widened (×2, ×3) distributions of fibre strength

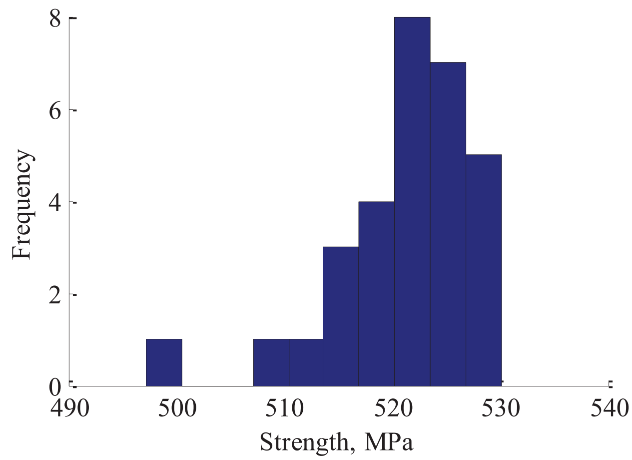

Figure 5. Final strength distribution (30 simulations, ELS fibre bundle model)

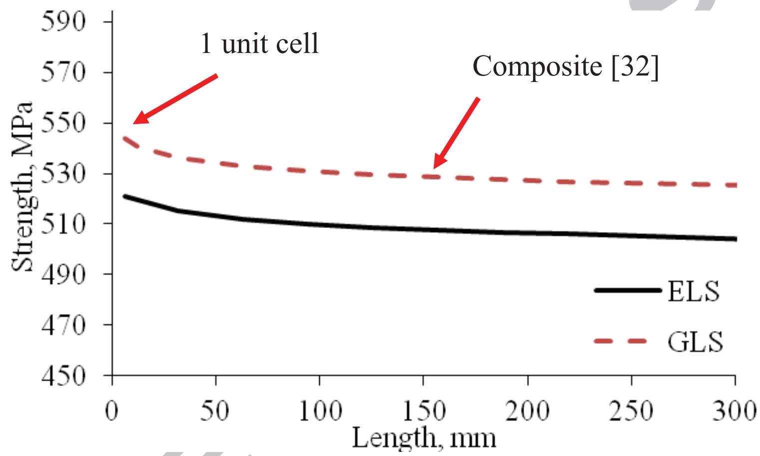

Figure 6. Average strength of the chain of unit cells

Table 1. Fibre and matrix properties

Fibre/matrix	$\bar{\sigma}_0$, MPa	L_0, mm	ρ	m	α	E_1^f, GPa	E_2^f, GPa	ν_{12}^f	ν_{23}^f	E_m, GPa	ν_m	σ_m, MPa
AS4/Epoxy [5]	4275.0	12.5	10.3	8.0	0.6	234	16.6	0.26	0.30	2.7	0.35	69.0
T700/Epoxy [22, 24]	5470.0	20.0	5.60	7.0	0.6	220	15.0	0.26	0.30	3.5	0.35	73.0

Table 2. Results of simulations for UD composites

	Vf, %	Length, mm	Experimental strength, MPa	Predicted strength, MPa			Rule of Mixtures, MPa
				ELS	ELS approx.	GLS	
AS4/Epoxy [5,32]	59	152	1890	1958±7	1957±8	2005±8	2337
T700/Epoxy [22]	70	20	3409±202	3189±55	3189±53	3358±49	3452